RAS 14378

Citizens Exhibit 60

Portions Deliberately Omitted
Only Included 77-85
Other Relevant Pages Submitted by
NRC Staff as Staff Exhibit 6

5. Sandbed Region Minimum Thickness Study

In addition to the stress and stability analysis of the drywell shell using the average UT measurements in the sandbed region (thicknesses described in Section 2.6, and analyses outlined in Sections 3 and 4), a minimum sandbed thickness study was also performed. These analyses aim to establish the minimum uniform thickness in the sandbed region that maintains compliance with the ASME B&PV code. The minimum acceptable shell thickness established here is based on a buckling (stability) analysis for the refueling load case. The refueling load case appears to govern the potential for instability since a relatively low effective factor of safety was produced in the average UT measurement analysis at 2.15. For Service Level B (refueling condition), a factor of safety of 2.0 is required by ASME N-284.

The previous GE analysis (GE, 1991b) assumed a uniform sandbed shell thickness of 0.736". Their analyses produced an applied compressive stress of 7.58 ksi in the sandbed region and an inelastic buckling stress of 21.30 ksi (per ASME N-284). This produces an effective factor of safety of 2.81. A subsequent calculation documented in a 1993 GPU Nuclear Calculation Sheet (GPU Nuclear, 1993) shows an applied compressive stress of 7.58 ksi in the sandbed region for a shell thickness of 0.736", but with a lower value for the inelastic buckling stress at 15.18 ksi. This produces an effective factor of safety of 2.0, or at the required ASME N-284 value.

The inconsistency between the two calculations appears to stem from a difference in the application of the increased capacity reduction factor due to the tensile stresses in the circumferential (hoop) direction. This issue was discussed in detail in the previous stability analysis section. Article 1500 of ASME N-284 states clearly that an increased capacity reduction factor may be justified if an internal pressure loading is present and causes tensile stresses in the circumferential direction. This internal pressure aids in "smoothing" the initial imperfections and increased the buckling capacity under compressive meridional stresses. The lack of an internal pressure load for the refueling load case prevents the justified use of an increased capacity reduction factor. As with the buckling calculations for the refueling load case in the previous section, the minimum thickness study does not employ any increase in the capacity reduction factor.

The shell thicknesses used in the minimum thickness study are summarized in Table 5-1 for regions outside of the sandbed region. The degraded thickness values for the majority of the drywell are equivalent to the values used in the average UT measurement analysis. The only exception being the thickness assigned to the lower sphere above an elevation of 15'-6.8", or the center of the ventlines. In this region of the lower sphere (see Figure 5-1), the thickness is set to 1.154", or the nominal as-built value. This remains consistent with inspections of the upper portions of the lower sphere. In the average UT measurement analysis, additional conservatism was introduced by degrading the entire lower sphere uniformly in each bay combination. However, several confirmatory analyses performed during this study showed that the thickness assigned to the lower sphere above elevation 15'-6.8" has only a negligible effect since the buckling occurs in the sandbed below 15'-6.8".

In the lower sphere below elevation 15'-6.8" (sandbed region), the drywell shell is set to a uniform thickness. This region is shown in Figure 5-1. While the same finite element mesh was used as for the average UT measurement analyses, the local thinned regions under the ventlines for Bays 1 and 13 are uniformly thinned consistent with the surrounding shell. In addition, this study only examined the minimum thickness required in the sandbed region and not in the upper portions of the sphere or in the cylinder.

Table 5-1. Main Drywell Shell Model Thicknesses Outside of Sandbed Region

Section	Original Thickness, in	Degraded Thickness, in	Section	Original Thickness, in	Degraded Thickness, in
Head	1.1875	N/C	Reinforcing Around Ventlines	2.875	2.618
Upper Cylinder	1.1875	N/C	Lower Sphere (below Sandbed)	1.154	N/C
Main Cylinder	0.640	0.585	Bottom Sphere	0.676	N/C
Knuckle	2.5625	2.54	Middle Sphere Thickened	1.0625	0.9625
Upper Sphere	0.722	0.676	Reinforcing Around Hatch	2.625	2.525
Middle Sphere	0.770	0.670	Lower Sphere (above El. 15'-6.8")	1.154	N/C

N/C – No Change

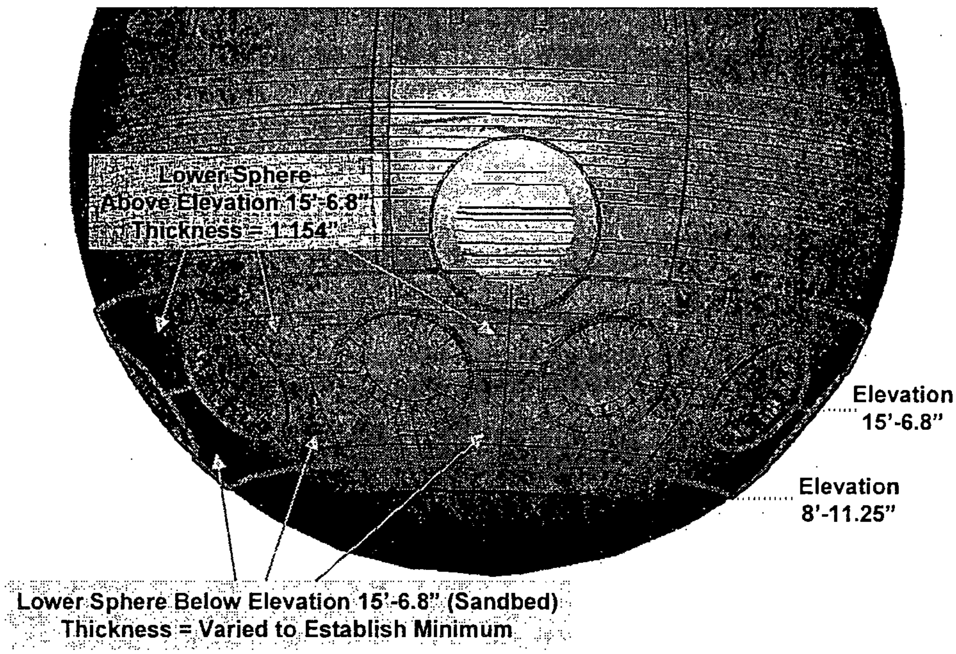

Figure 5-1. Drywell Lower Sphere for Establishing a Minimum Thickness in the Sandbed Region (Ventlines and Hatch Removed for Clarity)

The thickness values assigned to the sandbed region were varied from 0.800" up to 1.050" with a concentration of analyses performed between 0.800" and 0.860". In the previous buckling analysis section, a buckling analysis was also performed for the undegraded drywell containment which included a uniform thickness of 1.154" throughout the sandbed region. The results of each of these analyses are summarized in Figure 5-2. Here, the effective factor of safety is plotted against the associated shell thickness in the sandbed region. This study shows that a thickness of 0.844" is required in the sandbed region to produce an effective factor of safety equal to the ASME N-284 value of 2.0.

Figure 5-2 also plots the datapoint established in the previous buckling analysis section using average UT measurement data. In that analysis, the bay combination that buckled first was set to a thickness of 0.842" and resulted in an effective factor of safety equal to 2.15. Although the thicknesses used in the minimum thickness analysis and the average UT measurement analysis are essential equivalent, there are several important factors that produce the difference in safety factors. First, the average UT measurement analysis included two locally thinned regions that, in general, cause lower effective factors of safety for buckling in the adjacent bays than without the locally thinned regions. However, the effect of the locally thinned is outweighed by the existence of bay combinations with thickness far exceeding 0.842" (see Figure 2-32). For the average UT measurement analyses, 5 out of the 10 bay combinations were assigned thicknesses near or above 0.9". The existence of thicker bays enables a redistribution of the compressive loads leading to buckling. Therefore, the average UT measurement analysis produced an effective factor of safety of 2.15 with a thickness of 0.842", while the minimum thickness study produced an effective factor of safety of 2.0 with a thickness of 0.844". In the minimum thickness study, the entire sandbed region was uniformly thinned which prevents any redistribution of the load through thicker shell regions. The effect of the locally thinned regions was not rigorously explored in the average UT measurement analyses, but it is likely that the effective factor of safety of 2.15 would increase without the presence of the locally thinned region.

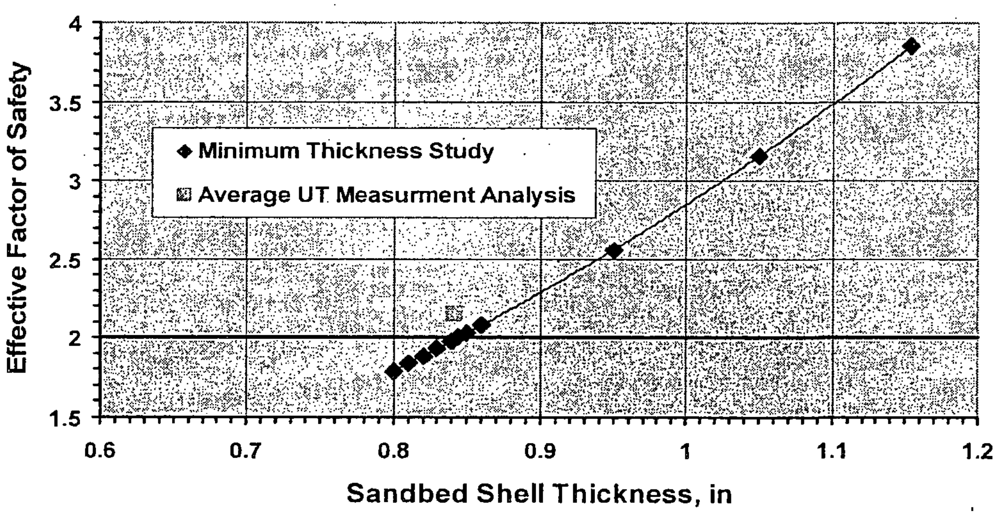

Figure 5-2. Effective Factor of Safety Values Computed for Various Thicknesses in the Sandbed Region for the Refueling Load Combination

Figure 5-3 and Table 5-2 illustrate the buckling location and ASME N-284 calculations for the sandbed with a thickness of 0.844". The major displacements for the first buckling mode in the sandbed are located between the ventline in Bays 1 and 3.

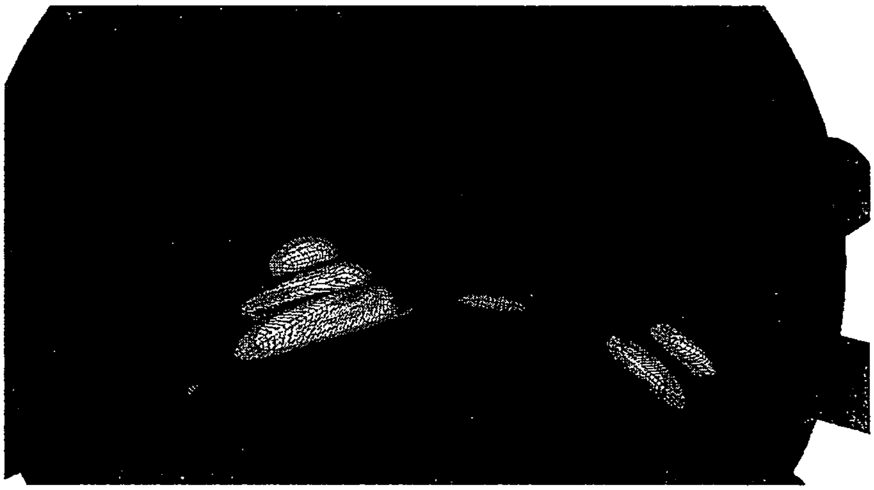

Figure 5-3. Buckling in the Sandbed Region with a Thickness of 0.844" for the Refueling Load Combination

Table 5-2. Buckling Evaluation for the Refueling Load Case with a Thickness of 0.844" in the Sandbed

Sphere Radius, in	420
Sphere Thickness, in	0.844
Material Yield Stress, ksi	38
Elastic Modulus, ksi	29500
Factor of Safety, FS	2
Applied Meridional Compressive Stress from Analysis, σ_c, ksi	4.78
Load Factor from Bucking Analysis, λ	9.67
Theoretical Elastic Buckling Stress, $\sigma_{ie} = \lambda\sigma_c$, ksi	46.19
Capacity Reduction Factor, α	0.207
Reduced Elastic Instability Stress, $\sigma_e = \alpha\sigma_{ie}$, ksi	9.56
Yield Stress Ration, $\Delta = \sigma_e/\sigma_y$	0.252
Plasticity Reduction Factor, η	1.0
Inelastic Instability Stress, $\sigma_i = \eta\sigma_e$, ksi	9.56
Allowable Compressive Stress, $\sigma_{all} = \sigma_i/FS$, ksi	4.78
Applied Compressive Stress Percentage of Allowable, σ_c/σ_{all} * 100	100.0%
Effective Factor of Safety, $FS_E = \sigma_i/\sigma_c$	2.00

6. Summary of Assumptions

The study performed for this program required a number of assumptions. A summary of the most significant assumptions is provided below.

- The Accident and Post-Accident load combinations are assumed to govern the stress analysis.

- The Refueling and Post-Accident load combinations are assumed to govern the buckling (stability) analysis.

- Information of the loads applied to the finite element model was taken from the previous study by GE. These loads were not independently verified.

- The seismic loading was applied using static coefficients provided in the Final Safety Analysis Report (FSAR, 2003). The static coefficients were applied using body forces in both the vertical and lateral directions. The displacement time histories (ground motions) were not made available for this study. The body forces used for the seismic loads were increased in the post-accident load combination to account for the mass of the water flooding the drywell.

- The ventlines were modeled down to the intersection with the ventline header. Here, springs acting in the radial and vertical directions were added to approximate the compliance of the ventline header. The spring constants were based on a simple submodel analysis of the ventline header. Since the ventline is connected to the torus with a flexible bellow, all interaction between the ventline and torus was neglected.

- The ventline jet deflector was modeled as a solid plate. In reality, the deflector has multiple holes throughout the plate. The thickness of the solid plate in the current model was reduced to account for the holes.

- In a number of cases, the exact location that a specific load acts upon the drywell shell was not known. The magnitude and elevation of these loads were provided in the GE report, but the azimuth locations remained unknown. In these cases (mainly in the case of the penetration loads), the loads were distributed along the entire circumference of the drywell as a surface traction.

- The loads applied to the drywell shell were "smeared" along a region defined on the shell surface. Typically, the region of application was taken as the area where an item is actually attached to the shell in the real structure. As mentioned above, the penetration loads were smeared along the entire circumference since loads for individual penetrations were not provided.

- The spacing of the upper and lower beam seats around the circumference is not constant, but the appropriate load distribution at each seat was not known. The loads for the upper and lower beam seats were distributed equally at each point of attachment to the drywell shell.

- The concrete that fills the drywell shell interior from an elevation of 8'-11.25" to 10'-3", and the additional curbs, have not been accounted for in this model. The drywell shell is assumed encased in concrete below elevation 8'-11.25" (bottom of sandbed).

- For the accident load combination, the internal 44 psi pressure and the thermal load of 292°F (starting at 70°F) were applied to the entire drywell shell down to an elevation of 8'-11.25". The concrete within the interior of the drywell shell extends up to 10'-3" with curbs extending up to 12'-3". Since the bond between the steel shell and the concrete is not known, it was assumed that a gap could exist which would enable gas to pressurize and heat the shell down to 8'-11.25", or the bottom of the sandbed region on the exterior of the shell. Even if no gap exists initially, it is likely that the initial pressurization (pressure << 44 psi) acting on the shell above elevation 10'-3" would cause a gap to open. This would allow heated gas to flow between the shell and concrete.

- The Personnel Lock & Equipment Hatch penetration geometry (extent modeled and thicknesses assigned) was approximated and the outer surface fixed against vertical displacement.

- The coefficient of thermal expansion for the A-212-61T Grade B pressure vessel steel used for the drywell was assumed to be 6.5E-6°F^{-1}.

- A number of assumptions were made to develop the thicknesses assigned to the model in its degraded state. Section 2.6 provides a detailed discussion of these items.

- A very limited mesh convergence study was performed which led to the use of a 4" nominal element size. It was assumed that this mesh size was acceptable even though all load combinations were not examined in the convergence study and no checks on buckling were performed using different mesh sizes. In addition, a 1" nominal mesh size was used in the two local regions under the ventlines in Bay 1 and 13. No checks were performed to assess the mesh size in these regions.

- Several assumptions were made in developing the ASME stress limits. These are discussed in Section 3..

- ASME Code Case N-284 was used to assess the stability of the degraded drywell shell. It was assumed that since the refueling case does not include any internal pressure, that the increase in buckling capacity used by GE for cases with circumferential (hoop) tension was not appropriate. Since the post-accident load case includes internal pressure, an increase in the capacity was applied.

7. Conclusions

The structural integrity of the degraded Oyster Creek drywell shell has been analyzed in this study. The allowable stresses and the buckling stability were both examined in accordance with the ASME B&PV code. The ASME allowable stresses are met for all three load cases examined here given the modeling and loading procedures outlined in Section 2. The only potential exception is for the primary plus secondary stresses located at the base of the sandbed region of the accident condition due to the thermal expansion of the shell. There are a number of modeling and loading assumptions in this region that may contribute to the stress magnitudes recorded in the current analysis. In addition, the primary plus secondary stresses were compared to the allowables use in the previous GE analysis (GE, 1991a). The current code does not require an evaluation of the primary plus secondary stresses for Service Level C. However, these stresses were assessed in this report to be consistent with the previous evaluation by GE. The buckling evaluation performed here using ASME N-284 show that based on the loadings and the model described in Section 2 both the refueling and post-accident load combinations met buckling requirements with a one exception. The buckling at the upper beam seat for the refueling load case with degradation does not meet the required factor of safety of 2. As described in Section 4, the potential constraint provided by the attached beam has not been included in this analysis. Table 7-1 summarizes the major conclusions for this study and for the previous GE analyses.

Table 7-1. Comparison of Conclusion Between GE Study (GE, 1991a and b) and the Current Study

Current Study Conclusion	GE Study Conclusion
The ASME B&PV stress analysis of the degraded Oyster Creek drywell shows all values within code limits. The current study uses average UT measurement data to assign thicknesses in the sandbed region. (Note that some primary plus secondary stresses for the accident condition are of concern as discussed in Section 3.)	The ASME B&PV stress analysis of the degraded Oyster Creek drywell shows all values within code limits. The GE study assumed a conservative uniform thickness of 0.736" in the sandbed region.
ASME B&PV Code Case N-284 stability analysis of the degraded Oyster Creek drywell shows that acceptable factors of safety are met. The current study uses average UT measurement data to assign thicknesses in the sandbed region. (Note that the buckling at the upper beam seats produces an effective factor of safety slightly less than 2 for the refueling load case, but this may be affected by the modeling of that specific detail.)	ASME B&PV Code Case N-284 stability analysis of the degraded Oyster Creek drywell shows that acceptable factors of safety are met. The GE study assumed a conservative uniform thickness of 0.736" in the sandbed region.
The minimum uniform shell thickness required to meet the ASME N-284 buckling safety factor was determined to be 0.844" in the sandbed region. This thickness was established using the buckling analysis for the refueling load case.	The minimum uniform shell thickness required to meet the ASME N-284 buckling safety factor was determined to be 0.736". This thickness was established using the refueling load case. (The thickness of 0.736" was established in a calculation by GPU Nuclear, 1993. This calculation included an increase in the capacity reduction factor not used in the current study.)

The assessments performed here employ a uniform thinning of the drywell shell over large sections of the surface. The thicknesses assigned in each region were based on limited measurement data since a very small percentage of the shell has been examined. In many cases, the raw data was not available. This led to the use of averages provided by AmerGen throughout the relevant documentation.

8. References

ABAQUS Analysis User's Manual, Version 6.5. 2004. Pawtucket, RI: Hibbit, Karlsson & Sorenson, Inc.

AmerGen April 4, 2006, Letter to U.S. NRC, 2130-06-20284, NRC Docket No. 50-219.

AmerGen April 7, 2006, Letter to U.S. NRC, 2130-06-20289, NRC Docket No. 50-219.

ASME (American Society of Mechanical Engineers). 2004. *Boiler and Pressure Vessel Code*. Sections III and VIII. New York, NY: American Society of Mechanical Engineers.

Cherry, J.L., and Smith, J.A., Capacity of Steel and Concrete Containment Vessels with Corrosion Damage, NUREG/CR-6707, SAND2000-1735, U.S. Nuclear Regulatory Commission, 2000.

Chicago Bridge & Iron (CB&I, 1980) Structural Drawings of the Oyster Creek Drywell, Torus, and Ventlines, attached to AmerGen letter to NRC, July 7, 2006, NRC Docket No. 50-219.

Final Safety Analysis Report (Updated), Oyster Creek Nuclear Generating Station (FSAR), AmerGen, Exelon, Revision 13, April 2003.

GE Stress Analysis Report, "An ASME Section VIII Evaluation of the Oyster Creek Drywell for Without Sand Case – Part I – Stress Analysis", GE Index #9-3, DRF #00664, February 1991a.

GE Stability Analysis Report, "An ASME Section VIII Evaluation of the Oyster Creek Drywell for Without Sand Case – Part II– Stability Analysis", GE Index #9-4, DRF #00664, February 1991b.

GPU Nuclear, Calculation Sheet, Oyster Creek Drywell External UT Evaluation, C-1302-187-5320-024, 1993.

Individual Plant Examination Submittal Report, Oyster Creek, (IPE), June 1992.

Johnson, B,G. editor, Guide to Stability of Design Criteria for Metal Structures, Third Edition, John Wiley & Sons, 1976.

Spencer, B.W., Petti, J.P., and Kunsman, D.M., Risk-Informed Assessment of Degraded Containment Vessels, NUREG/CR-6920, SAND2006-3772P, U.S. Nuclear Regulatory Commission, 2006.

Standard Review Plan for the Review of Safety Analysis Reports for Nuclear Power Plants (SRP), NUREG-0800, U.S. Nuclear Regulatory Commission, 1996.